NÖHÜ Müh. Bilim. Derg. / NOHU J. Eng. Sci., 2022; 11(3), 713-726

Niğde Ömer Halisdemir Üniversitesi Mühendislik Bilimleri Dergisi
Niğde Ömer Halisdemir University Journal of Engineering Sciences

Araştırma makalesi / Research article

www.dergipark.org.tr/tr/pub/ngumuh / www.dergipark.org.tr/en/pub/ngumuh

Mechanical and microstructural properties of cement mortars developed with different curing conditions and design parameters

Farklı kür koşulları ve tasarım parametreleri ile geliştirilen çimento harçlarının mekanik ve mikroyapısal özellikleri

Muhammet Güneş[1], Hasan Erhan Yücel[2,*], Hatice Öznur Öz[3]

[1,2,3] *Niğde Ömer Halisdemir University, Civil Engineering Department, 51240, Niğde Turkey*

Abstract

The aim of this study is the investigation of microstructural effects on cement mortars (CMs) of four different parameters as cement dosage, water/cement ratio, pozzolanic material and curing effect. To achieve the purpose of this study, SEM/EDX, XRD, FTIR and TGA/DTA analysis were performed. A total of 18 mixtures were produced and exposed to water curing (WC) and air curing (AC). In the design of these mixtures, three different cement dosages as 360, 400 and 450 kg/m^3 and three different water/cement ratios as 0.40, 0.45 and 0.50 were used. Silica fume (SF) was preferred to observe the effect on microstructural properties clearly of pozzolanic material. In addition, super plasticizer (SP) was utilized in all mixtures and kept constant as 12 kg/m^3. The compressive strength, flexural strength and ultrasonic pulse velocity (UPV) of these mixtures were determined at 28 and 90 days. Eight mixtures were chosen to observe the effect of four different parameters in a microstructural sense. XRD, SEM/EDX, FTIR and TGA/DTA analyses were applied to these mixtures. It can be said that microstructural analyses supported the findings obtained from mechanical tests.

Keywords: Microstructural properties, XRD, TGA/DTA, FTIR, Cement mortars

Öz

Bu çalışmanın amacı, çimento dozajı, su/çimento oranı, puzolanik malzeme ve kür etkisi olmak üzere dört farklı parametrenin çimento harçları (ÇH) üzerindeki mikroyapısal etkilerinin araştırılmasıdır. Bu amaca ulaşmak için SEM/EDX, XRD, FTIR ve TGA/DTA analizleri yapılmıştır. Toplam 18 karışım üretilmiş ve bu karışımlar su kürü (SK) ve hava kürüne (HK) maruz bırakılmıştır. Bu karışımların tasarımında 360, 400 ve 450 kg/m^3 olmak üzere üç farklı çimento dozajı ve 0,40, 0,45 ve 0,50 olmak üzere üç farklı su/çimento oranı kullanılmıştır. Puzolanik malzemenin mikroyapısal özellikler üzerindeki etkisini net olarak gözlemlemek için silis dumanı (SF) tercih edilmiştir. Ayrıca, tüm karışımlarda süper akışkanlaştırıcı (SA) kullanılmış ve 12 kg/m^3 olarak sabit tutulmuştur. Bu karışımların basınç dayanımı, eğilme dayanımı ve ultrasonik titreşim hızı (UTH) değerleri 28 ve 90 günde belirlenmiştir. Mikroyapısal anlamda dört farklı parametrenin etkisini gözlemlemek için sekiz karışım seçilmiştir. Bu karışımlara XRD, SEM/EDX, FTIR ve TGA/DTA analizleri uygulanmıştır. Mikroyapısal analizlerin, mekanik testlerden elde edilen bulguları desteklediği söylenebilir.

Anahtar kelimeler: Mikroyapısal özellikler, XRD, TGA/DTA, FTIR, Çimento harçları

1 Introduction

Some of the factors affecting the strength gain of cementitious composites are cement dosages, water/cement (w/c) ratio and curing. Moreover, the addition of a pozzolanic material to cement matrix directly affects the strength, depending on the amount of active silicon dioxide (SiO_2) in its content. In the last two decades, a great deal of research has been done on the effect of cement dosage [1,2], w/c ratio [3,4], curing method [5,6] and pozzolanic materials [7,8] on the strength development of cementitious composites. According to these researches, while the increase in cement dosage increased the basic mechanical properties, the increase in w/c ratio affected negatively [1-4]. Nevertheless, strength development of concretes subjected to water curing (WC) was much higher compared to air curing (AC) [5,6].

Cementitious composites incorporating several types of concretes and mortars are the most common construction and building materials used since the manufacture of cement. The main reason for using cement in these composites is that it reacts with water and provides strength since it has a hydraulic binding feature. İncrement in the strength can be explained with the Calcium-Silica-Hydrate (C-S-H, $C_3S_2H_3$) gels formed by the hydration of dicalcium silicate (C_2S) and tricalcium silicate (C_3S), which are the basic components of cement to provide C-S-H gels. The reaction of C_2S and C_3S are shown in Equation 1 and Equation 2, respectively as follows [9-14].

$$2C_2S+4H \longrightarrow C_3S_2H_3 + CH \quad (1)$$

$$2C_3S+6H \longrightarrow C_3S_2H_3 + 3CH \quad (2)$$

In addition to the reactions mentioned above, there may be different reactions where C-S-H gels are formed depending on the content of the cementitious composites

* Sorumlu yazar / Corresponding author, e-posta / e-mail: heyucel@ohu.edu.tr (H.E. Yücel)
Geliş / Recieved: 30.12.2021 Kabul / Accepted: 13.04.2022 Yayımlanma / Published: 18.07.2022
doi: 10.28948/ngmuh.1055199

[10]. For example, if a pozzolanic material is present in the cementitious mixture, a reaction occurs between active silica and calcium hydroxide (CH) [10]. This reaction, in which C-S-H gels are obtained, is stated below as Equation 3 [10].

$$CH+S+H \longrightarrow C\text{-}S\text{-}H \quad (3)$$

These complicated reactions occurring in cementitious composites directly affect the strength gain of the composites [14,15]. Therefore, knowing the mineralogical properties of the mixture and microstructural characteristics of the obtained composite can clearly reveal the effects of these reactions on strength development [14,15].

When the researches are examined in terms of the pozzolanic material, usually, the mechanical strength developed with the increment of the pozzolanic material amount in the cementitious composites [7,8]. Particularly, the positive effect of pozzolanic materials with high SiO_2 content, such as silica fume (SF), on the flexural strength and compressive strength was clearly seen [16-18]. SF is an amorphous (non-crystalline) and non-hazardous by-product material form silicon and Ferro-silicon alloy industry having ultra-fine particle size and large surface area which is suitable for concrete mix [16,19,20]. SF reacts with calcium hydroxide in the concrete mix to form stable calcium hydro silicates. According to research carried out by the authors of [21,22], silica fume does not affect C-S-H densities but does influence the chemical composition of the phase. At the same time, C-S-H phase thickening is observed with time. Fine particles of silica (nanosilica) significantly affect the acceleration of the hydration processes of clinker phases, as well as the amount of hydrated phases formed, especially during the first seven days of hydration [21,23]. Therefore, as seen in Equation 1 and 2, the amount of CH emerging as a by-product has also attracted the attention of the researchers owing to the contribution to the formation of C-S-H gel as given in Equation 3 [9-14]. Previous studies revealed that at 10–15% partial replacement of cement with SF can result in an increasing strength of concrete [18,24-26]. Benli [16,27] investigated the performance of mechanical properties of self-compacting mortars mixes with SF and fly ash and observed that 15% (5% fly ash and 10% SF) replacement of cement produced best compressive and flexural strengths. [16]. In other research, Duval and Kadri [28] indicated that partial replacement of SF up to 10% does not reduce the workability and also up to 20 percent SF content the maximum strength is obtained. Singh et al. [29] observed that when 5% and 10% of cement are replaced with SF, the maximum compressive strength is obtained by replacing 10% of SF. According to the literature studies, it can be clearly stated that SF increases the mechanical performance of concrete. However, investigating the effects of SF on the increase in strength in two different curing effects may be a privilege of this study.

In literature studies, important analysis techniques such as XRD, FTIR and TGA/DTA have been used to characterize the C-S-H and CH content and to investigate the potential and actual $CaCO_3$ (C) binding for the different mixtures of cementitious composites [30]. In addition, SEM/EDX is applied to determine the variations in microstructures. For example, Weerdt et al. [31] indicated that the Ca/Si ratio of ordinary Portland cement incorporating fly ash as pozzolanic material decreased compared to ordinary Portland cement while Al/Si ratio increased. Similarly, other literature studies showed that cement-based materials included the higher Al/Si and lower Ca/Si ratios in the presence of pozzolanic material after longer reaction times [31-36]. Moreover, at the end of XRD analysis performed by Awoyera et al. [37] were determined CH formed as result of hydration reaction between cement and water in cementitious materials can be provide for early strength gain in the cement paste, largely because of fast self-hydration of the cement. They reported that the reduction of the CH peaks in the cement matrix after 28 days can be explained with the pozzolanic reactions performed after the initial hydration reactions, in the presence of the pozzolanic material. Akça and Özyurt [38] used XRD analysis to determine the quantities of C-S-H, CH and C in concrete under different curing conditions. Moreover, in the same research, variations of CH and C content were determined with TGA/DTA analysis. Researchers observed that the effects of AC and WC conditions for CH and C contents changed in samples taken from the center and surface of the samples [38]. Du and Tan [39] indicated that CH consistently reduced in the cement matrix with increased pozzolanic material. Wang et al. [40] reported that mechanical and durability properties of the concrete incorporating SF developed and this development can be explained with the pozzolanic reactivity of SF, which is verified by FTIR at 3640 cm^{-1} revealed that chemical reactions between SF and CH. According to this information obtained from the literature, it was determined that the C-S-H and CH changes in cementitious composites with the addition of pozzolanic material were determined or the curing effects on CH and C were investigated. However, when different cement dosage and different water/binder ratio was used, the lack of scientific studies in the literature on how the CH and C contents change has been identified. In addition, it is considered that pozzolanic material behavior under different curing effect needs to be investigated with XRD, SEM/EDX, FTIR and TGA/DTA analysis. Therefore, it is very important to evaluate these parameters mineralogical by XRD analysis and to reveal their microstructural properties with SEM-EDX, FTIR and TGA/DTA analysis and to examine them in terms of hydration reactions.

Although the effects of the above-mentioned parameters on the basic mechanical tests such as flexural strength and compressive strength of cementitious composites were investigated in previous studies, there is no study evaluating the results in terms of microstructural and mineralogical characteristics. For this purpose, the mineralogical and microstructural properties of CMs, whose compressive and flexural strengths were investigated with four different parameters (cement dosages, w/c ratio, curing and pozzolanic material), were determined on selected eight mixtures.

2 Experimental Study

2.1 Materials

A total of 18 CMs developed in this study were composed of CEM I 42.5R type (ASTM Type I cement) ordinary Portland cement. The one of aims in this study was to determine how the pozzolanic material will exhibit its effect on strength development in two different curing effects. Therefore, it was thought that a single usage rate would be decisive in determining this difference. According to literature studies, it was determined that SF had a significant effect on strength development at 10% usage rate. Consequently, in the 9 CM mixture, SF was used as a pozzolanic material at a rate of 10%. The SEM images and physical and chemical properties of cement and SF are presented in Figure 1 and Table 1, respectively. As seen in Table 1, silica content of SF was determined as 68.64%. As it is known, silica content of SF is generally 90% and above. Therefore, the XRD analyses of both the SF used in this study and the SF with 91.85% silica content are given in Figure 2 together with the XRD analysis of the cement. According to the XRD results, it was determined that the SF used in this study had similar XRD patterns to SF incorporating 91.85% silica. Thus, it has been proven that the material used in this study is SF. However, the peak differences at 19, 28, 32 and 36 [°2θ] of the SF used in this study can be considered as a result of the fact that it contains less silica and more MgO, Na_2O and K_2O than that of the other SF. In addition, particle size distribution curves of materials used in the production of CMs are presented in Figure 3. Natural sand (0–4 mm) and crushed sand (0–2 mm) were used in the CMs. Specific gravities of these materials are 2.67 and 2.63, respectively. The natural sand from river was utilized to enhance the workability of HPM because of natural process of attrition tends to possess better shape and smoother surface texture. It also carries moisture that is trapped in between the particles. Crushed sand with angular, rough surface structure and low grain size (0–2 mm) was used to meet the strength requirement of CM. CMs contained 100% natural aggregates including 70% natural sand and 30% crushed sand by the total aggregate volume. For each volume concentration, a grading curve was generated to be used in the final mortar mixture regarding the regions recommended by TS 706 [41]. Liquid polycarboxylic ether-based super plasticizer (SP) with specific gravity of 1.07 and solid content of 40% was utilized to increase workability.

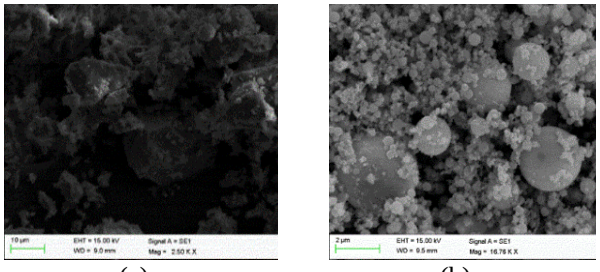

(a) (b)

Figure 1. SEM images of (a) cement and (b) SF

Table 1. The chemical and physical properties of cement and SF

Chemical Analysis (%)	Cement	SF
CaO	65.73	1.16
SiO_2	18.24	68.64
Al_2O_3	4.57	1.59
Fe_2O_3	2.89	1.54
MgO	1.87	9.63
K_20	0.79	3.11
Na_2O	0.25	4.00
P_2O_5	0.08	0.10
Mn_3O_4	0.07	0.15
TiO_2	0.28	-
Physical Properties	**Cement**	**SF**
Loss of Ignition	2.50	4.50
Specific Gravity	3.15	2.42
BET Analysis (m^2/kg)	431.29	2983.70

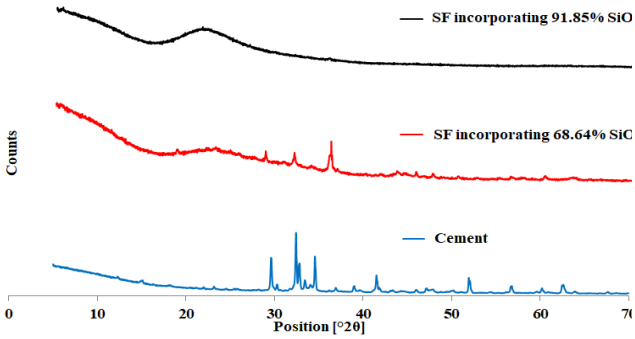

Figure 2. XRD analyses of cement and SF

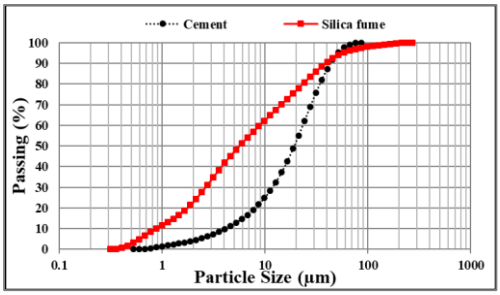

(a)

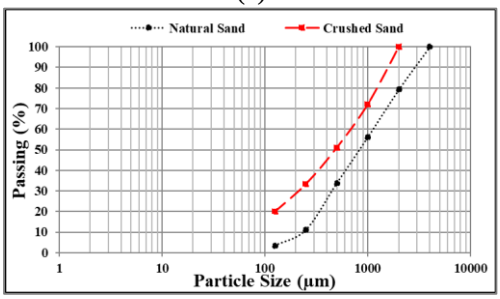

(b)

Figure 3. SEM images of (a) cement and SF and (b) natural sand and crushed sand

2.2 Production procedure and mixing proportions of CMs

A total of 18 CMs were produced and these mixtures were exposed to WC and AC. In the design of CM mixtures, three different cement dosages as 360, 400 and 450 kg/m^3 and three different w/c ratios as 0.40, 0.45 and 0.50 were determined. In addition, SF was preferred to investigate clearly the effects on microstructural properties of CMs of pozzolanic material. SP was utilized in all mixtures as 12 kg/m^3. Mixing proportions of CMs are given in Table 2. Codes of CMs were denoted depending on binder amount, water/binder ratio and SF content, respectively, For example; CM-360-0.4-10 mixture designed with 360 kg/m^3 cement and SF, 0.4 water/binder ratio and 10% SF (10% of binder content). CM mixtures were produced according to ASTM C305 [42].

2.3 Test procedures

2.3.1 Fresh and mechanical tests

The fresh properties of CMs were determined with slump flow diameter test according to ASTM C1437 [43]. Firstly, CMs were tamped 20 times after fill to half and all of the mold. Then, the surface of the CMs was levelled with a trowel. Finally, the table dropped 25 times in the 15 second, and the slump flow diameters of CMs were determined.

The mechanical behaviours of CMs were determined with flexural strength, compressive strength and ultrasonic pulse velocity (UPV) tests. Compressive strengths and flexural strengths of CMs were determined with respect to ASTM C349 [44] and ASTM C348 [45] at 28 and 90 days, respectively. The flexural strength tests of CMs were performed with three specimens in dimensions of 40x40x160 mm^3. Compressive strength tests of CMs were carried out on six specimens using prism pieces broken in flexural strength tests. The flat surfaces of the broken samples were placed in a special apparatus. Inside the special apparatus, there were two square pieces, one at the bottom and the other at the top of the apparatus, with a side length of 40 mm. The samples were placed between the parts inside this apparatus. Thus, sample was made to break into a cube with a length of 40 mm of one side. UPV test, performed on three specimens in the dimensions of 40x40x160 mm^3 was done accordance with ASTM C597 [46] at 28 and 90 days. UPV values along with flexural strengths and compressive strengths of CMs were determined with the average of test results.

2.3.2 SEM/EDX, XRD, TGA/DTA and FTIR analyses

To observe the effect of the design parameters on the microstructural analysis of CMs, the eight mixtures were determined. The morphological, mineralogical and microstructural performance characteristics of the CM-360-0.40-0-WC, CM-400-0.40-0-WC, CM-450-0.40-0-WC, CM-400-0.45-0-WC, CM-400-0.50-0-WC, CM-400-0.40-10-WC, CM-400-0.40-0-AC and CM-400-0.40-10-AC mixtures were determined with the aid of SEM/EDX, XRD, TGA/DTA and FTIR analyses. Morphological properties expressed shape and structure were investigated with SEM analysis. Since mineralogical properties indicate the compounds forming the structure, mineralogical properties of CMs were determined by EDX, XRD, TGA/DTA and FTIR analyses. Microstructural properties, on the other hand, include all these analyses since they express all the factors in the microstructure.

Table 2 Mixing proportions of CMs (kg/m^3)

Mix ID	water/ binder	Binder amount	Cement	SF	Water	Natural sand	Crushed sand	SP
CM-360-0.40-0	0.40	360	360	-	144	1367.6	577.3	12
CM-360-0.40-10	0.40	360	324	36	144	1361.1	574.6	12
CM-400-0.40-0	0.40	400	400	-	160	1313.9	554.7	12
CM-400-0.40-10	0.40	400	360	40	160	1306.7	551.6	12
CM-450-0.40-0	0.40	450	450	-	180	1246.9	526.4	12
CM-450-0.40-10	0.40	450	405	45	180	1238.8	523.0	12
CM-360-0.45-0	0.45	360	360	-	162	1333.9	563.1	12
CM-360-0.45-10	0.45	360	324	36	162	1327.5	560.4	12
CM-400-0.45-0	0.45	400	400	-	180	1276.6	538.9	12
CM-400-0.45-10	0.45	400	360	40	180	1269.4	535.9	12
CM-450-0.45-0	0.45	450	450	-	202.5	1204.8	508.6	12
CM-450-0.45-10	0.45	450	405	45	202.5	1196.7	505.2	12
CM-360-0.50-0	0.50	360	360	-	180	1300.3	548.9	12
CM-360-0.50-10	0.50	360	324	36	180	1293.8	546.2	12
CM-400-0.50-0	0.50	400	400	-	200	1239.2	523.1	12
CM-400-0.50-10	0.50	400	360	40	200	1232.0	520.1	12
CM-450-0.50-0	0.50	450	450	-	225	1162.8	490.9	12
CM-450-0.50-10	0.50	450	405	45	225	1154.7	487.5	12

CM-360-0.40-0-WC, CM-400-0.40-0-WC and CM-450-0.40-0-WC mixtures have been selected to determine the differences between different cement dosages. CM-400-0.40-0-WC, CM-400-0.45-0-WC and CM-400-0.50-0-WC mixtures have been used to observe the different w/b effect. CM-400-0.40-0-WC, CM-400-0.40-10-WC, CM-400-0.40-0-AC and CM-400-0.40-10-AC mixtures have been analysed to determine the effect of pozzolanic material under different curing conditions. In addition, CM-400-0.40-0-WC with CM-400-0.40-0-AC mixtures and CM-400-0.40-10-WC with CM-400-0.40-10-AC have been compared to observe the effects of WC and AC. While SEM analysis was performed, EDX was determined at area determined on the SEM analysis. The XRD scanning process was applied at steps of 0.013° and in the range of 10 to 70°. TGA analysis was performed in the range of 25 °C–1000 °C. 15 mg powered samples for TGA analysis was heated at nitrogen atmosphere with scanning rate of 10 °C/min. Typical FTIR frequency unit analysis was wave numbers (cm^{-1}). Analysis of the individual spectra in FTIR was determined with a chemical reaction in the specimen. The temperature and relative humidity in the FTIR analysis were 20 °C and 60%, respectively.

3 Results and discussions

3.1 Slump flow diameter

The results of slump flow diameters of a total of 18 CMs were presented in Figure 4. As seen in Figure 4, workability of CMs increased as a result of decreased aggregate amount due to increasing cement dosage at the same water/binder (w/b) ratios. For example, slump flow diameter of CM450-0.4-0 mixture was higher than that of CM400-0.4-0 and CM-360-0.4-0. Therefore, it can be said that a reduction in the aggregate content depending on increase of cement dosage leads to a reduction in the water content, which decreases the CMs' workability. In addition, it is known that as water increases in the cement based composites, the spacing of the fine materials grains increase. This increment in grain spacing of powder materials can improve the workability of mortar/concrete [47,48]. Therefore, for all CMs, when considered fixed cement dosages and SF contents, slump flow diameters of CMs increased with rise of w/b ratio. Exemplarily, workability of CM-360-0.5-0 was higher than that of CM-360-0.45-0 and CM-360-0.4-0. In addition, SF, another parameter of this study, increased partially the workability of CMs. For instance, slump flow diameters of CM-450-0.5-10, CM-400-0.5-10 and CM-360-0.5-10 mixtures was measured as 24.4, 20.7 and 17.5 while for CM-450-0.5-0, CM-400-0.5-0 and CM-360-0.5-0 mixtures, this values were determined as 22.7, 20.3 and 15.2, respectively. Incorporation of SF developed results of slump flow diameter because of its lubrication effect that would release water entrapped between small particles [15,49]. Moreover, this development in workability of CMs can be explained with the spherical micro-structure of SF presented in Figure 1. This spherical microstructure reduced inter-particle friction as a result of the particles act as small bearings [15,50,51]. Therefore, it can be said that all these results are in agreement with conclusions pointed out in previous studies.

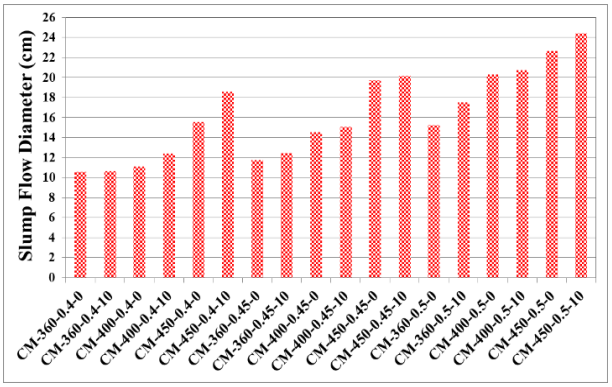

Figure 4. Slump flow diameters of CMs

3.2 Compressive and flexural strengths and ultrasonic pulse velocity (UPV)

The compressive strength, flexural strength and UPV test results of CMs exposed to WC and AC are shown in Figure 5, Figure 6 and Figure 7, respectively. As expected, the strength characteristics of the samples subjected to WC were higher than that of AC. However, the compressive strengths at 90 days of the mixtures exposed to WC were 14.5%-22.1% higher than the compressive strengths at 28 days. These values for mixtures exposed to AC were determined as 10.1%-23.8%. Similarly, in study investigating the effect of SF on the compressive strength of concrete by Duman [52], was determined that the 90-day compressive strength of the mixtures was 10.3%-46.2% higher than the 28-day compressive strength. Compressive strength, flexural strength and UPV values of CMs changed in parallel to each other. For constant w/b ratio and constant SF content (CMs with/without SF), with the increase of cement dosage improved the mechanical properties of CMs at 28 and 90 days. Exemplarily, for both WC and AC, strength characteristics of CM-450-0.4-10 were higher than that of CM-400-0.4-10 and CM-360-0.4-10. The increase in cement content increased the hydration reaction and the resulting hydration product. Moreover, the use of more cement reduced the porosity of CMs. When mixtures having constant cement and SF (with/without) content was evaluated, it can be clearly said that the increase in w/b ratio reduced the strength characteristics and UPV values of CMs for both WC and AC. For example, compressive strength of CM-450-0.4-0 was higher than that of CM-450-0.5-0 in the ratios of 11.9% and 12.3% at 28 and 90 days for WC, respectively. For AC, these values were calculated as 15% and 7.7% at 28 and 90 days, respectively. As a result of the increase in the water content of CMs, hydration products had greater difficulty to fill the space between the cement grains [47,48]. This increment in porosity decreased the mechanical performance and UPV values of CMs [53]. Bentz and Aitcin [54] and Dowell and Cramer [55] expressed that water to cement ratio had adverse relation with strength. Some other investigators stated have that strength characteristic of concrete developed with reducing water to cement ratio [56-

60]. In addition, 10% SF content in CMs increased the flexural and compressive strengths along with UPV values compared to CMs produced without SF at 28 and 90 days. For WC, this development changed in the range of 4.4-9.8% and 5.3-8.4% at 28 and 90 days, respectively. For AC, these values were in the range of 6.9-12.6% and 5.2-10.0% at 28 and 90 days, respectively. Similar to these results, in the study conducted by Özcan [61] using different w/b ratios, the compressive strength of concrete containing 10% SF compared to the control concrete was found to be higher in the ranges of 3.8%-20% at 28 days and 4.3%-22.5% at 90 days for WC. Moreover, at different w/b ratios, the compressive strength of the mixture containing 10% SF for AC at 28 and 90 days was higher than that of the control mixture in the ranges of 10.8%-30.5% and 11.5%-30.2%, respectively. In addition, Özcan [61] stated that this strength improvement continued for both different w/b ratios and different curing methods in the use of 10% SF at 180 days. According to these results, the physical and chemical effects of SF provided a significant improvement in compressive strength. Strength increase performed under both curing conditions in the presence of SF can be explained with pozzolanic characteristic and fineness of SF. The pozzolanic reactions between CH occurring from hydration of cement and amorphous SF formed C-S-H (calcium-silicate-hydrate) gels [15, 51]. In addition, as seen in Table 1, fineness of SF mineral (2983.70 kg/m^3) was much higher than that of cement (431.29 kg/m^3). This micro-fine mineral increased the packing of solid materials and decreased the porosity by filling spaces between cement grains [15, 62].

3.3 SEM/EDX

The eight samples of 18 mixture exposed to WC and AC were selected to observe the effect of the design parameters on the mineralogical and microstructural properties of CMs. Figure 8 shows the results obtained from the SEM/EDX scanning. Ca/Si ratios of these eight samples were given in Table 3. As seen in Figure 8 and Table 3, Ca/Si ratios of CM-360-0.40-0-WC, CM-400-0.40-0-WC, CM-450-0.40-0-WC, CM-400-0.45-0-WC, CM-400-0.50-0-WC and CM-400-0.40-0-AC mixtures were almost equal to each other. According to this result, different cement dosage and w/b ratio of CMs exposed to different two curing effect did not change the Ca/Si ratio in the CMs due to the elemental contents of the materials forming the matrix for these six samples were the same. Therefore, it can be said that increasing or decreasing the cement dosage and w/b ratio in CM, or curing in water/air of the mixtures may be affected positively or negatively the reactions in the matrix, but does not changed the elemental ratios in the total mass. However, the inclusion of a different material in the cement matrix can affect chemical reactions or change the ratio of Ca/Si in the total mass. As stated in the Table 3, Ca/Si ratios of CM-400-0.4-10-WC and CM-400-0.4-10-AC were lower than that of CM-400-0.4-0-WC and CM-400-0.4-0-AC, respectively. This can be explained with higher SiO_2 content of SF used instead of cement as seen in Table 1. In addition, the Ca/Si ratio of the CM-400-0.4-10 mixture containing 10% SF and exposed to two different curing effect, was very close to each other. Therefore, it can be said that different curing types effected chemical reactions but, did not affect the mineralogical structure of the materials in cement matrix.

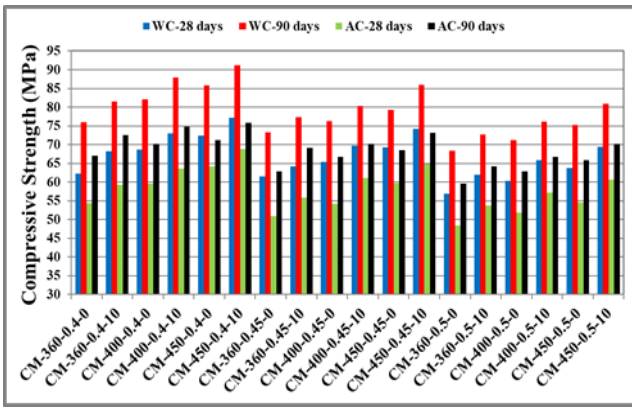

Figure 5. Compressive strengths of CMs

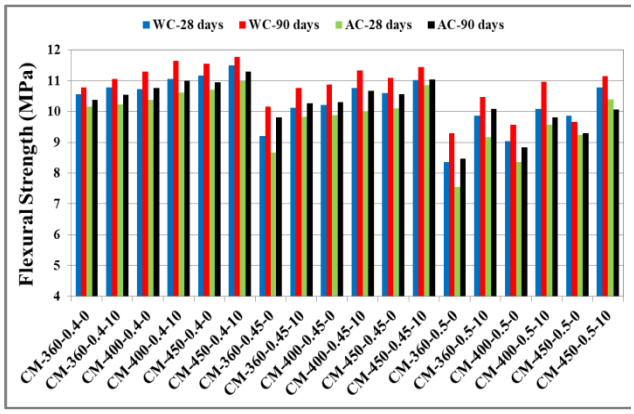

Figure 6. Flexural strengths of CMs

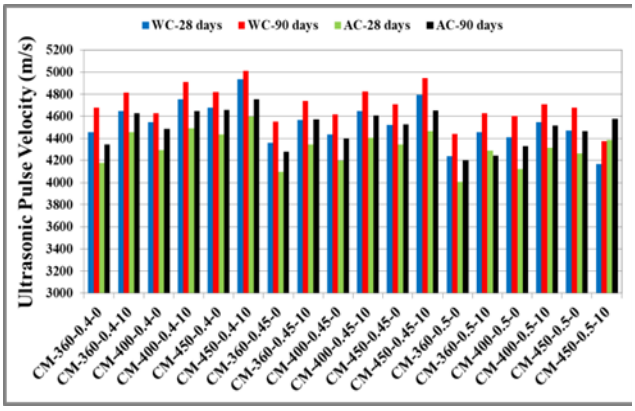

Figure 7. UPV values of CMs

3.4 XRD

The XRD analyses of the selected eight mixtures for 90 days are given in Figure 9. As seen in Figure 9, the peak (around 29.5 °2θ) showed the C-S-H and $CaCO_3$ (C) components is exactly the same. For this reason, the evaluation of XRD results was made based on the peaks (around 18.0 and 33.7 °2θ) showed $Ca(OH)_2$ (CH) content instead of C-S-H. The CH contents of CM-360-0.40-0-WC,

CM-400-0.40-0-WC and CM-450-0.40-0-WC mixtures given in Figure 8 increased depending on increasing cement content. This increase can be explained by the formula presented in Equation (1,2). According to these formulas, the CH content in the mortar/concrete increases in parallel with the increase in strength ($C_3S_2H_3$). Therefore, it can be said that the increment in the cement content increased the CH content of the CMs as well as rising the strength. The effect of changing w/b ratio on the CH content of cement mortar was determined with the help of CM-400-0.40-0-WC, CM-400-0.45-0-WC and CM-400-0.50-0-WC. As seen in Figure 8, the w/b ratio had no significant effect on the CH content of the CMs. Two different curing effects on the CH content of CMs were investigated with CM-400-0.40-0-WC and CM-400-0.40-0-AC. According to the results, the CH content of mixture exposed to AC was lower than that of WC. Similarly, the CH content of CM-400-0.40-10-AC was lower than that of CM-400-0.40-10-WC. This situation can be explained by the fact that the reaction in WC can be developed faster thanks to the water in the environment and thus the hydration products (C-S-H and CH) are more. Therefore, both the strength and CH content of the CMs exposed to WC were higher than AC. It can be said that SF reduced the CH content of CMs for both curing conditions. The CH content of CM-400-0.40-10-WC and CM-400-0.40-10-AC was lower than that of CM-400-0.40-0-WC and CM-400-0.40-0-AC, respectively. It is known that the chemical reactions between CH formed as a result of cement hydration with amorphous SF, form C-S-H gels [15,51]. In addition, the presence in the cement paste of SF mineral form smaller CH crystals, accelerates the reactions and induces several nucleation sites for precipitation of the hydration products [15,63]. Therefore, SF increased strength characteristics, also reduced the CH content in cement matrix.

Table 3. Ca/Si ratios, $Ca(OH)_2$ (CH, %) and $CaCO_3$ (C, %) contents of CMs

Mix ID	SEM/EDX	TGA/DTA	
	Ca/Si	$Ca(OH)_2$ (CH,%)	$CaCO_3$ (C,%)
CM-360-0.40-0-WC	2.01	0.60	16.63
CM-400-0.40-0-WC	1.99	0.77	16.01
CM-450-0.40-0-WC	1.99	0.82	16.19
CM-400-0.45-0-WC	1.94	0.74	16.63
CM-400-0.50-0-WC	1.98	0.75	17.74
CM-400-0.40-10-WC	1.59	0.43	16.34
CM-400-0.40-0-AC	1.95	0.50	15.15
CM-400-0.40-10-AC	1.57	0.26	15.45

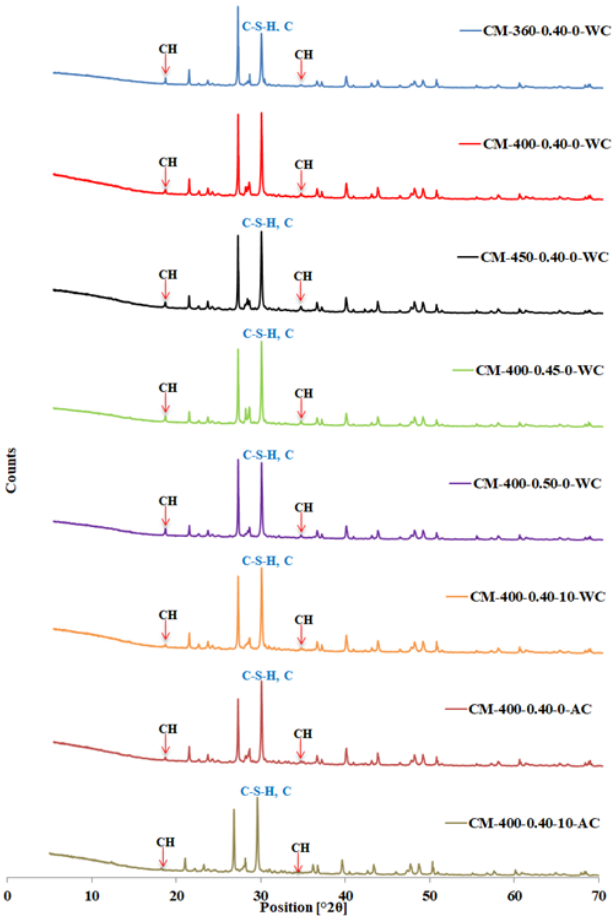

Figure 9. XRD analyses of determined eight mixtures

3.5 TGA/DTA

The results obtained from the TGA and DTA analysis should be considered to better understand the pozzolanic reactions and hydration kinetics of the CMs [64]. The portlandite content in CMs could be determined thinking the theoretical mass losses from the mass losses calculated from the TGA charts (Figure 10) between approximately peaks corresponding to 400 °C-460 °C temperatures (initial-final) in the DTA charts (Figure 10) [65] Therefore, the weight corresponding to 460 °C was subtracted from the weight corresponding to 400 °C in the TGA diagrams and the CH contents given in Table 3 of the mixtures were determined. Note that, when CH in cement matrix is decomposed to H_2O and CaO (burnt lime), the theoretical mass loss by the evaporation of the water was calculated [65]. It is an important curiosity issue how the content of CH has changed with increasing cement dosage, varying w/b ratios and different curing conditions. In addition, the change of CH content for both different curing effect in the cement paste over time, was utilized to quantify the chemical reaction of SF [66]. TGA/DTA analysis could be utilized to identify the hydration degree of cement via CH decomposition [66].

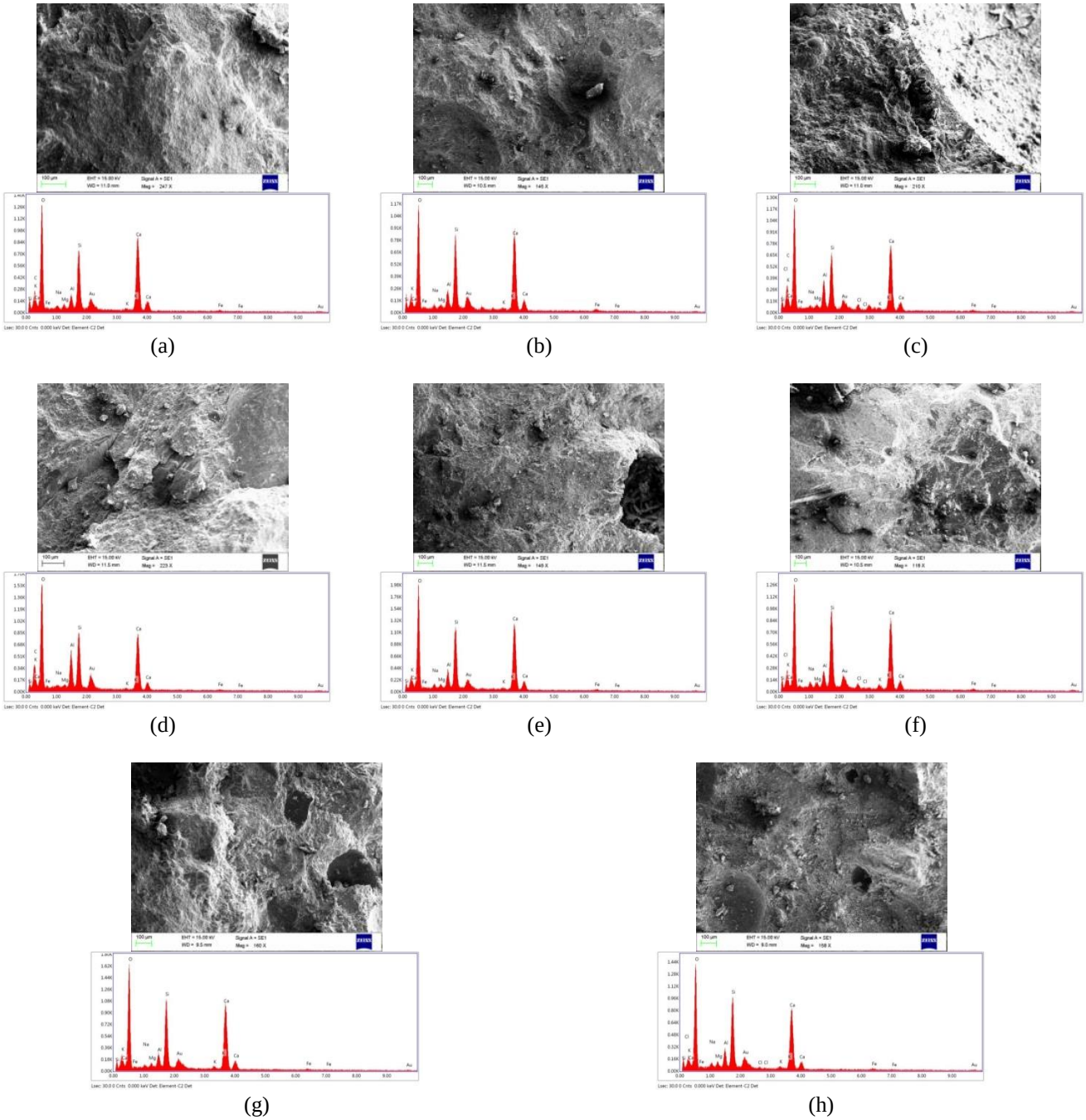

Figure 8. SEM images EDX results of a) CM-360-0.40-0-WC, b) CM-400-0.40-0-WC, c) CM-450-0.40-0-WC, d) CM-400-0.45-0-WC, e) CM-400-0.50-0-WC, f) CM-400-0.40-10-WC, g) CM-400-0.40-0-AC, h) CM-400-0.40-10-AC

Table 3 and the sharpness of DTA peaks in the range of 400-460 °C in Figure 10 (a, b, c) indicated that the CH content of CM-450-0.40-0-WC mixture were higher than that of CM-400-0.40-0-WC. The lowest CH content between these three mixtures was obtained from the CM-360-0.40-0-WC mixture. According to these results and the mechanical test results, based on the increased cement dosage, the CH contents of CMs increased, as well as the strengths. This can be explained by the hydration reaction of C_3S and C_2S presented in Equation (1) and Equation (2). As seen in Equation (1) and Equation (2), the increase in the amount of C_3S and C_2S reacted in cement matrix has been increased the CH content together with the C-S-H gel formed as a result of the reaction.

Graphical representations of CM-400-0.40-0-WC, CM-400-0.45-0-WC and CM-400-0.50-0-WC mixtures preferred to evaluate the effect of w/b ratio were shown in Figure 10 (b,d,e) and calculated CH contents of these three CMs were listed in Table 3. The CH contents of these three mixtures were very close to each other. Therefore, it can be said that no affecting the CH content in CMs of the increase/decrease in the w/b ratio. However, it was described in the section of

mechanical properties that the increased w/b ratio reduced strength characteristics. Therefore, this decrease can be attributed to porosity caused by increased water content and was not related to the content of CH. The effects of WC and AC on the CH contents of CMs were investigated with CM-400-0.40-0-WC and CM-400-0.40-0-AC mixtures given TGA/DTA curves in Figure 10 (b,g). Table 3 indicated that CH contents of these two samples were 0.77% and 0.50%, respectively. Similarly, when CM-400-0.40-10-WC and CM-400-0.40-10-AC (Figure 10 (f,h)) mixtures containing SF are also compared to each other in terms of CH contents, it was observed that CM subjected to the AC had a lower CH content. The lower CH content amount of CM exposed to AC can be attributed to much more hydration products formed the faster hydration reaction result in the WC. When Equation (1) and Equation (2) was considered, it can be said that there is more C-S-H gels of CM-400-0.40-0-WC, due to included more CH as a result of increased hydration product. Thus, the higher mechanical performances of CMs exposed to WC can be explained micro structurally more effectively. In addition, the weight loss because of CH decomposition of hydration products by TGA/DTA analysis was utilized to measure the amount of pozzolanic reaction [66]. The CH content of the CM-400-0.40-10-WC shown in Figure 10 (b,f) was much lower than that of the CM-400-0.40-0-WC. Similarly, the CH content of the CM-400-0.40-10-AC shown in Figure 10 (g, h) is much lower than that of the CM-400-0.40-0-AC. When the TGA/DTA analysis were evaluated, it can be seen that CH in CM-400-0.40-0-WC and CM-400-0.40-0-WC was 0.77% and 0.50% while CH in CMs incorporating 10% SF was 0.43% and 0.26%, respectively. Presence in the lower amount of CH in CMs incorporating SF can be the result of chemically bonding of the CH thanks to much more silica content (%68.64 given in Table 1) in chemical composition of SF [15].

It is known that decarbonation of carbonates in mortar/concrete began after 600 °C [51,68]. DTA peaks of a mortar/concrete sample for approximate 700 °C present $CaCO_3$ (C) decarbonation [69-72]. After 800 °C, weight loss of mortar/concrete slows down and also, most of the components in mortar/concrete become decomposed [67]. TGA/DTA curves given in Figure 10 have been confirmed the information above. The C contents of CMs were determined with the mass losses calculated from the TGA graphics approximately in the range of 600 °C-800 °C (initial-final) temperatures of the corresponding to peaks in the DTA graphics. Therefore, the weight corresponding to 600 °C was subtracted from the weight corresponding to 800 °C in the TGA diagrams and the C contents given in Table 3 of the mixtures were determined. When the values given in Table 3 for Figure 10 (a,b,c) were examined, it can be said that the cement dosage did not have a significant effect on carbonation. XRD and TGA/DTA analyses showed that the CH content of CMs changed in parallel with the cement content in the matrix. Therefore, the C content of CMs not being parallel to the cement dosage can be attributed to the C ensuing from C-S-H carbonation in the cement paste. The values given in Table 3 for Figure 10 (b,d,e) showed that the C content of the CMs increased with rising w/b ratio. In the XRD and TGA/DTA analysis, it was determined that the water content did not have a significant effect on the CH content. The increased C with increment in water content may be the result of the carbonation of C-S-H. When the CM-400-0.40-0-WC and CM400-0.40-10-WC (Figure 10(b,f)) were compared, it can be said that SF was slightly increased carbonation. Similarly, when Figure 10 (g) and Figure 10 (h) were compared, the partial increment for carbonation of CM containing SF was observed. Considering that the mixtures incorporating SF have less CH content, it can also be thought to increase the carbonation caused by C-S-H due to increased C-S-H in the cement matrix. Effects of WC and AC cures on carbonation of CMs were evaluated via CM-400-0.40-0-WC and CM-400-0.40-0-AC or CM-400-0.40-10-WC and CM-400-0.40-10-AC. According to XRD and TGA/DTA analyses, CH content of the mixtures subjected to AC was lower than that of other mixtures. In addition, the lower strength characteristics of the mixtures subjected to AC can be explained by the fact that less C-S-H formed as a result of slowing hydration due to the absence of water in the environment. Therefore, the degree of carbonation for AC was lower due to the mixtures exposed to AC contained less CH and C-S-H.

3.6 FTIR

FTIR spectrum can be thought as a graphic of transmittance and/or infrared light absorbance as a function of wavelength and/or frequency. When infrared light passes through the sample, all of functional group ensures the spectra to resonate at the characteristic absorption frequencies. The chart results define chemical reaction between the molecules [73]. It is known that, approximate 3643 cm^{-1} wave number in FTIR spectra represents the CH redient of mortar/concrete. Therefore, as seen in Figure 11, 3600-3700 cm^{-1} wavelength range of FTIR spectra was presented to investigate CH changes of the eight mixtures [74]. FTIR spectra showed that CH changes of the mixes supported the results obtained from XRD and TGA/DTA analyses. In accordance with the formula given in Equation 1 and Equation 2, the increased amount of cement increased the CH content in cement matrix. The CH content of CM-450-0.40-0-WC was higher than that of CM-400-0.40-0-WC and CM-360-0.40-0-WC, respectively. According to FTIR spectra of CM400-0.40-0-WC, CM-400-0.45-0-WC and CM400-0.50-0-WC, increased water content for constant cement dosage did not have a significant effect on the quantity of CH. When the pozzolanic material was used in CM, FTIR spectra were in agreement with TGA/DTA curves and XRD patterns. Namely, CH peak in the FTIR spectrum of the CM-400-0.40-0-WC and CM-400-0.40-10-WC with hydration reactions accelerated thanks to water curing was higher than that of CM-400-0.40-0-AC and CM-400-0.40-10-AC, respectively. The CH peaks of the CM-400-0.40-0-WC and CM-400-0.40-0-AC mixtures were sharper than that of the CM-400-0.40-10-WC and CM-400-0.40-10-AC mixtures, respectively. FTIR spectrum clearly indicated that, the increased amount of SF in CM reduced the CH content by the pozzolanic reaction.

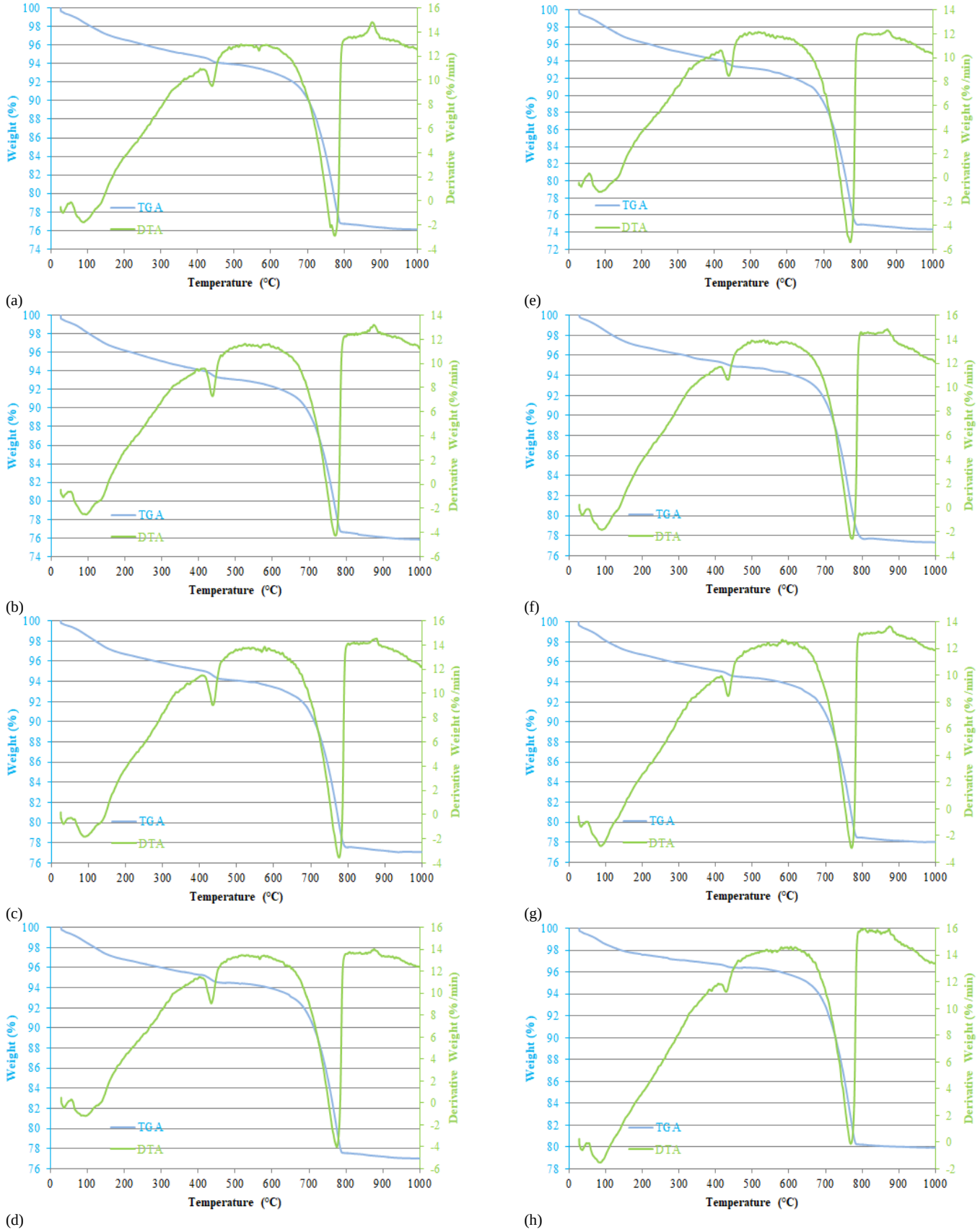

Figure 10. TGA and DTA results of a) CM-360-0.40-0-WC, b) CM-400-0.40-0-WC, c) CM-450-0.40-0-WC, d) CM-400-0.45-0-WC, e) CM-400-0.50-0-WC, f) CM-400-0.40-10-WC, g) CM-400-0.40-0-AC, h) CM-400-0.40-10-AC

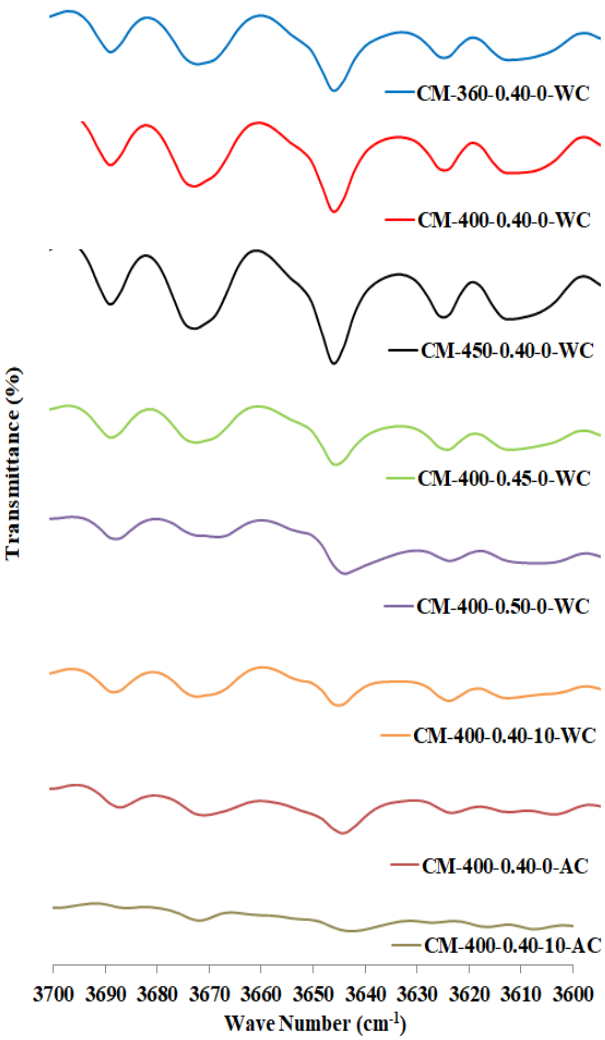

Figure 11. FTIR analyses of determined eight mixtures

4 Conclusions

The following findings from this study were obtained. The workability of CMs increased with the increment of cement dosage, w/b ratio and SF content. The mechanical properties of CMs improved due to acceleration the hydration reactions with increased cement content. However SEM/EDX indicated that Ca/Si ratio did not change significantly. XRD, FTIR and TGA/DTA analysis indicated that the CH content in the matrix changed in compatible with the improvement in strength with increased cement dosages. In addition, TGA/DTA showed that the cement dosage did not have an important influence on C variation.

The strength characteristics of CMs decreased as a result of increased porosity with the increment of w/b ratio. However, SEM/EDX analysis indicated that Ca/Si ratio almost keep steady. According to XRD, TGA/DTA and FTIR analyses, the w/b ratio had no important influence on the CH content of the CMs. Moreover, TGA/DTA showed that the C contents of the CMs increased with increment of w/b ratio.

XRD, TGA/DTA and FTIR demonstrated that the CH content of mixture exposed to WC was higher than that of AC In addition the degree of carbonation in the WC was higher than that of AC.

The CH contents of CMs incorporating SF were higher than that of CMs without SF. Therefore, SF increased strength characteristics. TGA/DTA analysis demonstrated that SF was slightly increased the carbonation.

References

[1] A. Ergün, G. Kürklü, M. S. Başpınar and M. Y. Mansour, The effect of cement dosage on mechanical properties of concrete exposed to high temperatures. Fire Safety Journal, 55, 160–167, 2013. https://doi.org/10.1016/j.firesaf.2012.10.016.

[2] R. Şahin, R. Demirboğa, H. Uysal and R. Gül, The effects of different cement dosages, slumps and pumice aggregate ratios on the compressive strength and densities of concrete. Cement and Concrete Research, 33, 1245–1249, 2003. https://doi.org/10.1016/S0008-8846(03)00048-6.

[3] O. Lotfi-Omran, A. Sadrmomtazi and I. M. Nikbin, A comprehensive study on the effect of water to cement ratio on the mechanical and radiation shielding properties of heavyweight concrete. Construction and Building Materials, 229, 116905, 2019. https://doi.org/10.1016/j.conbuildmat.2019.116905.

[4] V. G. Haach, G. Vasconcelos, and P. B. Lourenço, Influence of aggregates grading and water/cement ratio in workability and hardened properties of mortars. Construction and Building Materials, 25, 2980–2987, 2011. https://doi.org/10.1016/j.conbuildmat.2010.11.011.

[5] S. A. Alabi and J. Mahachi, Compressive strength of concrete containing palm oil fuel ash under different curing techniques. Materials Today: Proceedings, 43 (2), 1969–1972, 2021. https://doi.org/10.1016/j.matpr.2020.11.426.

[6] C. M. Yun, R. Rahman, C. Y. W. Phing, A. W. M. Chie and M. K. B. Bakri, The curing times effect on the strength of ground granulated blast furnace slag (GGBFS) mortar. Construction and Building Materials, 260,120622, 2020. https://doi.org/10.1016/j.conbuildmat.2020.120622.

[7] S. H. V. Mahalakshmi and V. C. Khed, Experimental study on M-sand in self-compacting concrete with and without silica fume. Materials Today: Proceedings, 27, 1061–106, 2020. https://doi.org/10.1016/j.conbuildmat.2020.120622.

[8] A. Mehtaa and D. K. Ashish, Silica fume and waste glass in cement concrete production: A review. Journal of Building Engineering, 29, 10088, 2020. https://doi.org/10.1016/j.jobe.2019.100888.

[9] X. Y. Wang and H.-S. Lee, Modeling the hydration of concrete incorporating fly ash or slag. Cement and Concrete Research, 40, 984–996, 2010. https://doi.org/10.1016/j.cemconres.2010.03.001.

[10] V. G. Papadakis and S. Tsimas, Effect of supplementary cementing materials on concrete resistance against carbonation and chloride ingress. Cement and Concrete Research, 30, 291–299, 2000. https://doi.org/10.1016/S0008-8846(99)00249-5.
[11] V. G. Papadakis, C. G. Vayenas and M. N. Fardis, Physical and chemical characteristics affecting the durability of concrete, ACI Materials Journal, 88, 186–196, 1991. http://www.concrete.org/Publications/InternationalConcreteAbstractsPortal.aspx.aspx?m=details&i=1993.
[12] V. G. Papadakis, Effect of fly ash on Portland cement systems, Part I: low calcium fly ash. Cement and Concrete Research, 29, 1727–1736, 1999. https://doi.org/10.1016/S0008-8846(99)00153-2.
[13] V. G. Papadakis, Experimental investigation and theoretical modeling of silica fume activity in concrete. Cement and Concrete Research, 29, 79–86, 1999. https://doi.org/10.1155/2014/102392.
[14] V. G. Papadakis, Effect of fly ash on Portland cement systems, Part II: high calcium fly ash. Cement and Concrete Research, 30, 1647–1654, 2000. https://doi.org/10.1016/S0008-8846(00)00388-4.
[15] S. Wang, L. Baxter and F. Fonseca, Biomass fly ash in concrete: SEM, EDX and ESEM analysis. Fuel, 87, 372–379, 2008. https://doi.org/10.1016/j.fuel.2007.05.024.
[16] M. Sharma, P. Behera, S. Saha, T. Mohanty and P. Saha, Effect of silica fume and red mud on mechanical properties of ferrochrome ash based concrete. Materials Today: Proceedings, in press. https://doi.org/10.1016/j.matpr.2021.11.372.
[17] S. Saha, P. Saha and T. Mohanty, Mechanical properties of fly ash and ferrochrome ash based geopolymer concrete using recycled aggregate. Recent Development in Sustainable Infrastructures, 75, 417–426, 2019. https://doi.org/10.1007/978-981-15-4577-1_34.
[18] A. Sikder and P. Saha, Effect of bacteria on performance of concrete/mortar: A review, International Journal of Recent Technology and Engineering, 7 (6C2), 12-17, 2019.
[19] L. Jianyong and T. Pei, Effect of slag and Silica fume on mechanical properties of high strength concrete. Cement and Concrete Research, 27 (6), 833–837, 1997. https://doi.org/10.1016/S0008-8846(97)00076-8.
[20] T. C. Holland, Silica fume user's manual. Silica fume Association, Report no FHWA-IF-05-016, 2005.
[21] M. Gruszczyński and M. Lenart, Durability of mortars modified with the addition of amorphous aluminium silicate and silica fume. Theoretical and Applied Fracture Mechanics, 107, 102526, 2020. https://doi.org/10.1016/j.tafmec.2020.102526.
[22] A. C. A. Muller, K. L. Scrivener, J. Skibsted, A. M. Gajewicz, and P. J. McDonald, Influence of silica fume on the microstructure of cement pastes: New insights from 1H NMR relaxometry. Cement and Concrete Research, 74, 116–125, 2015. https://doi.org/10.1016/j.cemconres.2015.04.005.
[23] J. I. Tobón, J. J. Payá, M. V. Borrachero and O. J. Restrepo, Mineralogical evolution of Portland cement blended with silica nanoparticles and its effect on mechanical strength, Construction and Building Materials, 36, 736–742, 2012. https://doi.org/10.1016/j.conbuildmat.2012.06.043.
[24] F. V. Ajileye, Investigations on micro-silica (silica fume) as partial cement replacement in concrete. Global Journal of Research in Engineering, 12, 17–24, 2012. https://engineeringresearch.org/index.php/GJRE/article/view/575.
[25] A. Mathew, Effect of silica fume on strength and durability parameters of concrete. International Journal of Engineering Sciences & Emerging Technologies, IJESET 3, 28–35, 2012.
[26] D. King, The effect of Silica fume on the properties of concrete as defined in concrete society report 74. cementitious materials, in: 37th Conference on Our World in Concrete & Structures, 29–31, 2012.
[27] A. Benli, Mechanical and durability properties of self-compacting mortars containing binary and ternary mixes of fly ash and silica fume. Structural Concrete, 20, 1096–1108, 2019. https://doi.org/10.1002/suco.201800302.
[28] R. Duval and E. H. Kadri, Influence of silica fume on the workability and the compressive strength of high-performance concretes. Cement and Concrete Research 28 (4), 533–547, 1998. https://doi.org/10. 1016/S0008-8846(98)00010-6.
[29] S. Singh, G. D. Ransinchung and P. Kumar, Effect of mineral admixtures on fresh, mechanical and durability properties of RAP inclusive concrete. Construction and Building Materials, 156, 19–27, 2017. https://doi.org/10.1016/j.conbuildmat.2017.08.1 44.
[30] Z. Shi, B. Lothenbach, M. R. Geiker, J. Kaufmann, A. Leemann, S. Ferreiro and J. Skibsted, Experimental studies and thermodynamic modeling of the carbonation of Portland cement, metakaolin and limestone mortars. Cement and Concrete Research, 88, 60–72, 2016. https://doi.org/10.1016/j.cemconres.2016.06.006.
[31] K. D. Weerdt, M. B. Haha, G. L. Saout, K. O. Kjellsen, H. Justnes and B. Lothenbach, Hydration mechanisms of ternary Portland cements containing limestone powder and fly ash. Cement and Concrete Research, 41, 279–291, 2011. https://doi.org/10.1016/j.cemconres.2010. 11.014.
[32] K. Luke and E. Lachowski, Internal composition of 20-year-old fly ash and slag blended ordinary Portland cement pastes. Journal of American Ceramic Society, 91, 4084–4092, 2008. https://doi.org/10.1111/j.1551-2916.2008.02783.x.
[33] J. I. Escalante-Garcia and J. H. Sharp, The chemical composition and microstructure of hydration products in blended cements. Cement and Concrete Composites, 26, 967–976, 2004. https://doi.org/10.1016/j.cemconcomp.2004.02.036.
[34] A. M. Harrisson, N. B. Winter and H. F. W. Taylor, An examination some pure and composite Portland cement

pastes using scanning electron microscopy with X-ray analytical capability. 8th ICCC, pp. 170–175, Rio de Janeiro, Brasil, 1986.
[35] P. L. Rayment, The effect of pulverised-fuel ash on the C/S molar ratio and alkali content of calcium silicate hydrates in cement. Cement and Concrete Research, 12, 133–140, 1982. https://doi.org/ 10.1016/0008-8846(82)90001-1.
[36] H. F. W. Taylor, K. Mohan and G. K. Moir, Analytical study of pure and extended Portland cement pastes: II, fly ash- and slag-cement pastes. Journal of American Ceramic Soc. 68, 685–690, 1985. https://doi.org/10.1111/j.1151-2916.1985.tb10125.x.
[37] P. O. Awoyera, J. O. Akinmusuru, A. R. Dawson, J. M. Ndambuki and N. H. Thom, Microstructural characteristics, porosity and strength development in ceramic-laterized concrete. Cement and Concrete Composites, 86, 224–237, 2018. https://doi.org/ 10.1016/j.cemconcomp.2017.11.017.
[38] A. H. Akca and N. Özyurt, Effects of re-curing on microstructure of concrete after high temperature exposure, Construction and Building Materials, 168, 431–441, 2018. https://doi.org/10.1016/j.conbuildmat. 2018.02.122.
[39] H. Du and K. H. Tan, Properties of high volume glass powder concrete. Cement and Concrete Composites, 75, 22–29, 2017. https://doi.org/10.1016/j.cemconcomp.2016.10.010.
[40] L. Wang, S. H. Zhou, Y. Shi, S. W. Tang and E. Chen, Effect of silica fume and PVA fiber on the abrasion resistance and volume stability of concrete. Composites Part B: Engineering, 130, 28–37, 2017. https://doi.org/10.1016/j.compositesb.2017.07.058.
[41] TS 706 EN 12620-A1, Aggregates for concrete. Institute of Turkish Standards, 2009.
[42] ASTM C305, Standard practice for mechanical mixing of hydraulic cement pastes and mortars of plastic consistency. Annual book of ASTM standards, 2017.
[43] ASTM C1437, Standard test method for flow of hydraulic cement mortar. Annual book of ASTM standards, 2017.
[44] ASTM C349, Standard test method for compressive strength of hydraulic–cement mortars (using portions of prisms broken in flexure). Annual book of ASTM standards, 2017.
[45] ASTM C348, Standard test method for flexural strength of hydraulic–cement mortars. Annual book of ASTM standards, 2017.
[46] ASTM C597, Standard test method for pulse velocity through concrete. Annual book of ASTM standards, 2016.
[47] J. B. Robertson and M. T. Ley, Determining the water to cement ratio of fresh concrete by evaporation. Construction and Building Materials, 242, 117972, 2020. https://doi.org/10.1016/j.conbuildmat.2019.11 7972.
[48] T. C. Powers and T. Willis, The air requirement of frost resistant concrete. In High. Res. Board Proceedings, 1950.
[49] Z. Wu, C. Shi and K. H. Khayat, Influence of silica fume content on microstructure development and bond to steel fiber in ultra-high strength cement-based materials (UHSC). Cement and Concrete Composites, 71, 97–109, 2016. https://doi.org/10.1016/j.cemcon comp.2016.05.005.
[50] S. Mindess, J.F. Young, and D. Darwin, Concrete. second ed., Prentice Hall, Pearson Education, USA, 2003 NJ 07458.
[51] T. K. Erdem and Ö. Kırca, Use of binary and ternary blends in high strength concrete. Construction and Building Materials, 22, 1477–1483, 2008. https://doi. org/10.1016/j.conbuildmat.2007.03.026.
[52] R. Duman, Silis dumaninin betonun performansına ve klor geçirimliliğine etkilerinin incelenmesi. Sakarya Üniversitesi, Fen Bilimleri Enstitüsü, Yüksek Lisans Tezi, 2010.
[53] S. H. Kosmatka, B. Kerkhoff and W. C. Panarese, Design and control of concrete mixtures. The Portland Cement Association, 2011.
[54] D. P. Bentz and P. C. Aitcin, The hidden meaning of water–cement ratio. Concrete International, 30 (5), 51–54, 2008.
[55] A. Dowell, and S. Cramer, Field measurement of water–cement ratio for Portland cement concrete – Phase II Field evaluation and development; Final Report. University of Wisconsin – Madison, Department of Civil and Environmental Engineering. Wisconsin Highway Research Program, 2002.
[56] B. Felekoğlu, S. Türkel and B. Baradan, Effect of water/cement ratio on the fresh and hardened properties of self-compacting concrete. Building and Environment, 42 (4), 1795–1802, 2007. https://doi. org/10.1016/j.buildenv.2006.01.012.
[57] R. Siddique, P. Aggarwal and Y. Aggarwal, Influence of water/powder ratio on strength properties of self compacting concrete containing coal fly ash and bottom ash. Construction and Building Materials, 29, 73–81, 2012. https://doi.org/10.1016/j.conbuildmat. 2011.10.035.
[58] N. S. Apebo and A.J. Shiwua, Effect of water-cement ratio on the compressive strength of gravel – crushed over burnt bricks concrete. Civil and Environmental Research, 3 (4), 74–81, 2013.
[59] I. M. Nikbin, M. H. A. Beygi, M. T. Kazemi, J.V. Amiri, S. Rabbanifar, E. Rahmani and S. Rahimi, A comprehensive investigation into the effect of water to cement ratio and powder content on mechanical properties of self compacting. Construction and Building Materials, 57, 69–80, 2014. https://doi.org/ 10.1016/j.conbuildmat.2014.01.098.
[60] L. R. Kumar, M. Karthikeyan and R. Raghu, Influence of water-cement ratio on compressive strength of burnt bricks. IOSR Journal of Mechanical and Civil Engineering 14 (2), 91–94, 2017.
[61] F. Özcan, Silis dumanı içeren harç ve betonların özellikleri ve hızlandırılmış kür ile dayanım tahmini. Çukurova Üniversitesi, Fen Bilimleri Enstitüsü, Yüksek Lisans Tezi, 2005.

[62] D. Pedro, J. de Brito and L. Evangelista, Evaluation of high-performance concrete with recycled aggregates: use of densified silica fume as cement replacement. Construction and Building Materials, 147, 803–814, 2017. https://doi.org/10.1016/j.conbuildmat.2017.05.007.

[63] ACI Committee 234, 234R-06, Guide for the use of silica fume in concrete, (2006) Michigan, USA https://www.concrete.org/publications/internationalconcreteabstract sportal/m/details/id/16670.

[64] H. K. Kim and H.K. Lee, Hydration kinetics of high-strength concrete with untreated coal bottom ash for internal curing. Cement and Concrete Composites 91, 67–75, 2018. https://doi.org/10.1016/j.cemconcomp.2018.04.017.

[65] J. Dweck, P. M. Buchler, A. C. V. Coelho and F. K. Cartledge, Hydration of a Portland cement blended with calcium carbonate. Thermochimica Acta, 346 (1–2), 105–113, 2000. https://doi.org/10.1016/S0040-6031(99)00369-X.

[66] I. Pane and W. Hansen, Investigation of blended cement hydration by isothermal Calorimetry and thermal analysis. Cement and Concrete Research, 35 (6), 1155–1164, 2005. https://doi.org/10.1016/j.cemconres.2004.10.027.

[67] D. N. Crook and M. J. Murray, Regain of strength and firing of concrete, Magazine and Concrete Research, 22 (6), 149–154, 1970.

[68] M. Henry, K. Hashimoto, I. S. Darma and T. Sugiyama, Cracking and chemical composition of cement paste subjected to heating and water re-curing. Journal of Advanced Concrete Technology, 14, 134–143, 2016.

[69] A. H. Akca and N. Özyurt, Effects of re-curing on residual mechanical properties of concrete after high temperature exposure. Construction and Building Materials, 159, 540–552, 2018. https://doi.org/10.1016/j.conbuildmat.2017.11.005.

[70] E. Menendez and L. Vega, Analysis of the behaviour of the structural concrete after the fire at the Windsor Building in Madrid. Fire Materials, 34, 95–107, 2010. https://doi.org/10.1002/fam.1013.

[71] F. Branda, G. Luciani, A. Costantini and C. Piccioli, Interpretation of the thermogravimetric curves of ancient pozzolanic concretes. Archaeometry, 43, 447–453, 2001. https://doi.org/10.1111/1475-4754.00027.

[72] G. Villain, M. Thiery and G. Platret, Measurement methods of carbonation profiles in concrete: thermogravimetry, chemical analysis and gamma densimetry. Cement and Concrete Research, 37, 1182–1192, 2007.

[73] H. E. Yücel and S. Özcan, Strength characteristics and microstructural properties of cement mortars incorporating synthetic wollastonite produced with a new technique. Construction and Building Materials, 223, 165–176, 2019. https://doi.org/10.1016/j.conbuildmat.2019.06.195.

[74] V. Bulatovic´, M. Melešev, M. Radeka, V. Radonjanin and I. Lukic´ , Evaluation of sulfate resistance of concrete with recycled and natural aggregates. Construction and Building Materials, 152, 614–631, 2017. https://doi.org/10.1016/j.conbuildmat.2017.06.161.